# A novel one-step wet denitration method by hydrodynamic cavitation and chlorine dioxide

Jingang Yang [a,1], Liguo Song [a,1,*], Yuhang Wei [a], Hao Sui [a], Chengqi Deng [a], Bohao Zhang [a], Kaixuan Lu [a], Minyi Xu [a], Zhitao Han [a], Xinxiang Pan [a,b]

[a] *Marine engineering college, Dalian Maritime University, Dalian, Liaoning 116026, China*
[b] *Guangdong ocean university, Zhanjiang, Guangdong 524088, China*

## ARTICLE INFO

## ABSTRACT

Ships have brought substantial economic benefits, and meanwhile, they release exhaust gases, including plenty of nitrogen oxides ($NO_x$). Increasingly stringent air pollutant emission standards (e.g., MARPOL) for ships have been established at home and abroad to reduce the pollution of $NO_x$. In this paper, a promising technology for removing $NO_x$ from ship exhaust by hydrodynamic cavitation (HC) and chlorine dioxide ($ClO_2$) was proposed. The mechanism of HC promoting denitration was discussed. The various influencing factors of the HC enhancing $ClO_2$ circulation denitration, such as the pressure difference ($\Delta P$) between the inlet and outlet of the HC reactor, solution temperature (10.0 – 55.0 °C), NO initial concentration (500–1000 ppm), gas flow rate (1.0–1.6 L/min), solution pH (3.00 – 11.00), and $ClO_2$ concentration (0.001–0.100 mmol/L) on denitration effect were studied in the experiments, in which the optimal conditions were established. On the basis of the results of HC enhancing $ClO_2$ circulation denitration, HC enhancing $ClO_2$ non-circulation denitration experiments were carried out. The results showed that the NO and $NO_x$ removal efficiencies reached 93% and 90%. We also measured the final anions in solutions after denitration by ion chromatography and discussed the reaction pathways.

## 1. Introduction

The continuous growth of world seaborne trade makes rapid growth in the global fleet. As of 30th October 2019, there were 96,295 ships with more than 100 gross tons worldwide. Ships bring substantial economic benefits [1]. Nevertheless, they also cause severe air pollution problems [2]. The exhaust gas from ships contains pollution sources such as particulate matter (PM), sulfur oxides ($SO_x$), and $NO_x$, which have adverse effects on the atmospheric environment and human health [3–7]. In response to ship pollution, increasingly stringent air pollutant emission standards (e.g., MARPOL) for ships have been established at home and abroad [8]. Scholars have studied many emission reduction technologies for the above reasons, finding that removing $SO_x$ and PM from ship exhaust is easy, but it is challenging to remove $NO_x$. Denitration is the key to the integrated treatment of ship exhaust.

Currently, there are many methods to reduce $NO_x$ emission from ships, such as selective catalytic reduction (SCR) [9–11], exhaust gas recirculation (EGR) [12–14], and wet denitration [15,16]. The denitration rate of the SCR system reached 80%− 95% [17]. However, due to the burning of low-quality fuels, the particles in ship exhaust are more likely to pollute the catalyst, causing catalyst poisoning, which is not conducive to the SCR system's operation. Moreover, the SCR system using urea or ammonia has an excellent practical effect on land, but considering the reality of the ship, putting a large amount of urea or ammonia in the living area harms the crew's life, which is another complex problem in the application of this technology on board. The EGR system can satisfy the Tier III standard for $NO_x$ emissions from ships, but it will lead to cylinder liner wear and increase exhaust products (e.g., PM and CO) [18]. The EGR system also has significant changes to the original engine structure, making it challenging to apply on existing ships in service.

The SCR and EGR only remove $NO_x$ in exhaust emissions; however, wet denitration technology can simultaneously remove various pollutants in the exhaust gas [18], which attracts the attention of researchers. $SO_x$ and PM can be effectively removed by wet denitration, while NO, which accounts for over 90% of $NO_x$ in ship exhaust, is hard to dissolve

---

in water [19], which brings challenges to wet denitration [20–22]. For meeting the challenges, multi-step wet denitration technology is investigated. Anette et al. [23] first used gaseous $ClO_2$ to oxidize NO to $NO_2$, then absorbed $NO_2$ with $Na_2SO_3$ and $Na_2CO_3$ solution, and the removal efficiency of $NO_x$ reached more than 90%. Although the denitration efficiency of the multi-step wet denitration technology is high, the multi-step wet denitration system is complicated and occupies an ample space, which does not apply to the ship with limited space. For solving the complexity of the wet denitration process, one-step wet denitration technology is investigated. In 2020, Xiao et al. [24] proposed a micro-nano bubble (MNB) oxidation-absorption process based on sodium humate for simultaneous desulfurization and denitration. MNBs are tiny bubbles less than 50 μm in diameter [6,7,25], which increases the gas-liquid contact area. The collapse of MNBs can produce hydroxyl radicals (•OH) to further facilitate the removal of NO [24,26]. The results showed that the removal efficiency of NO could reach more than 91.1%. Biological treatment is a new method for the removal of $NO_x$. Mao et al. [27] proposed a method by biological trickling filter for the removal of NO and $SO_2$. The results showed that the highest $NO_x$ removal efficiency was 60.2%. Biological treatment by nitrifier-enriched-activated-sludge (NAS) technology is expected to improve $NO_x$ removal efficiency. Sepehri et al. [28,29] proposed and proved that the enrichment of nitrifying bacteria could be achieved in NAS. They also found that a Chlorella vulgaris and NAS consortium could enhance nutrient removal and reduce metabolite generation [30]. Jin et al. [21] and Deshwal et al. [31] dissolved $ClO_2$ gas in water to directly remove $NO_x$ in a bubbling reactor, and the $NO_x$ removal efficiency was 66–72%. Furthermore, Deshwal et al. [32] used acidic $NaClO_2$ solution to remove $NO_x$ from the simulated flue gas. Their results showed that $ClO_2$, an intermediate product, participated in the oxidation and absorption of $NO_x$ under acidic conditions, and the highest denitration rate reached 81%. The one-step wet denitration system is simple, but it is not easy to achieve a denitration efficiency exceeding 90%. Research on a one-step denitration system with small space occupation and high denitration efficiency is a hot topic in ship air pollution control.

HC is a hydrodynamic phenomenon that occurs when the liquid pressure suddenly drops below the vapor pressure and then increases. When the local pressure of the liquid drops suddenly, the molecules in the weak part of the liquid are pulled apart, forming cavities. The water will vaporize and enter the cavities since the pressure is below the saturated vapor pressure. When the pressure rises sharply, the cavities are compressed adiabatically, producing ultra-high temperature (1000–15000 K) and ultra-high pressure (10–500 MP) and eventually collapse [33–39]. When cavities collapse, microjets can be formed to enhance local mass transfer. The cavitation process can also cause hydrolysis, producing •OH [33,40,41]. Chemical reactions can be accelerated by the extreme chemical reaction environment created by cavitation [35,40,42,43]. Cavitation has been used in biofuel refining and wastewater treatment and achieved remarkable results. In addition, Oxidant $ClO_2$ is safe, environmentally friendly, low in cost [44], and has a robust oxidizing property [45,46], which is beneficial to the oxidation and absorption of $NO_x$. Therefore, a novel one-step wet denitration method by HC enhancing $ClO_2$ is proposed in this paper. HC reactor can effectively improve wet denitration efficiency and reduce the equipment footprint. The denitration system mainly includes pumps, pipelines, and venturi injectors in practical applications. It takes up a small space suitable for ships with limited space.

We aim at the basic study of treatment theory and technology of removing $NO_x$ by HC enhancing $ClO_2$. Effects of the $\Delta P$, solution temperature, NO initial concentration, gas flow rate, solution pH, and $ClO_2$ concentration on the denitration effect were studied during the HC enhancing $ClO_2$ circulation denitration experiments, in which the optimal experimental conditions were established. On the basis of the results of HC enhancing $ClO_2$ circulation denitration, HC enhancing $ClO_2$ non-circulation denitration experiments were carried out. We also measured the final anions in solutions after denitration by ion chromatography and discussed the reaction pathways.

## 2. Experimental section

### 2.1. Experimental materials

The experimental setup included a gas feeding system, an HC reactor unit, and a flue gas analysis system (Fig. 1). The gas feeding system consisted of NO ($1000 \times 10^{-6}$ mol/mol and $3000 \times 10^{-6}$ mol/mol, balance with $N_2$), $N_2$ (purity≥99.999%), and mass flow controllers (MFC, Beijing Sevenstar Electronics Co., Ltd) controlling the gas flow rate, and a mixing chamber. The HC reactor unit mainly consisted of a constant temperature water bath keeping the solution temperature constant, 12.0 L of high purity $ClO_2$ solution ($ClO_2$, 11.12 mmol/L, purity≥99.99%, Guangzhou ZLDL Materials Technology Co., Ltd, Guangdong, China.) and pure water (18.2 MΩ·cm at 25.0 °C) in the thermostat bath tank as denitration solution, a venturi injector (model 384, Mazzei Injector Company, LLC, Bakersfield, USA.) as the HC reactor, and an injection pump (model: LSP02–2B, Baoding Longer Precision Pump Co., Ltd.) as a continuous syringe. 1 mol/L $H_2SO_4$ solution and 1 mol/L NaOH solution were used to adjust the solution's initial pH value. The solution pH was measured by Mettler-Toledo s210 SevenCompact™ pH during experiments. The reaction samples were analyzed by Thermo Scientific DIONEX ICS-600 ion chromatography (Dionex Ionpac™ AS23). $ClO_2$ in samples was detected by a UV spectrophotometer (UV-1800, Shimadzu, Japan). A turbine flow transducer (LWGY-10, Jinhu Heshi Instrument Co., Ltd., China) was used for measuring the liquid flow rate. The phantom v2012 high-speed camera with 10,000 fps was used to take photographs of the bubbles at the HC reactor outlet. The flue gas analysis system included an electronic condenser and a gas analyzer (Gasboard-3000UV, Hubei Cubic-Ruiyi Instrument Co., Ltd.). The electronic condenser cooled the flue gas and removed moisture for weakening the corrosion of the gas analyzer. The gas analyzer measured the concentrations of NO, $NO_2$, and $NO_x$.

### 2.2. Experimental procedures

Before each experiment, high-purity $N_2$ was used to empty the air in the pipeline. The denitration solution in the constant temperature water bath was drawn by the pump, and the solution was driven to flow through the line. Whether the solution flowed through the HC reactor was controlled by adjusting valves i and j. The experiment system worked either in the circulation denitration mode or non-circulation denitration mode.

The device was in the circulation denitration mode when valves c, d, e, g, h, j opened and valves a, b, f, i closed. The HC reactor inlet pressure ($P_i$) and outlet pressure ($P_o$) were adjusted by valves d and h. The liquid level of the first stage gas-liquid separator was controlled by valve g. When the denitration solution quickly passed through the HC reactor, a suction pressure was generated, which sucked the mixed gas into the HC reactor, and then a large number of Gas-Filled-Bubbles would be formed in the HC reactor. The bubbles and denitration solution flowed through the HC reactor and entered the first stage gas-liquid separator. The separated gas mixture passed through the second gas-liquid separator, the electronic condenser, and the gas analyzer in sequence. Simultaneously, the liquid flowed through valve e and then returned to the constant temperature water bath.

The HC enhancing $ClO_2$ non-circulation denitration was an optimization of the HC enhancing $ClO_2$ circulation denitration. During the non-circulation denitration experiment, valves b, d, f, g, h, j opened, and valves e, i closed. Valves a, c controlled whether the gas passed through the HC reactor. The continuous syringe injected $ClO_2$ solution into the pipeline at a constant rate. The $ClO_2$ solution and the NO mixture were simultaneously sucked into the HC reactor and reacted. After the gas-liquid separation, the solution entered the beaker through valve f.
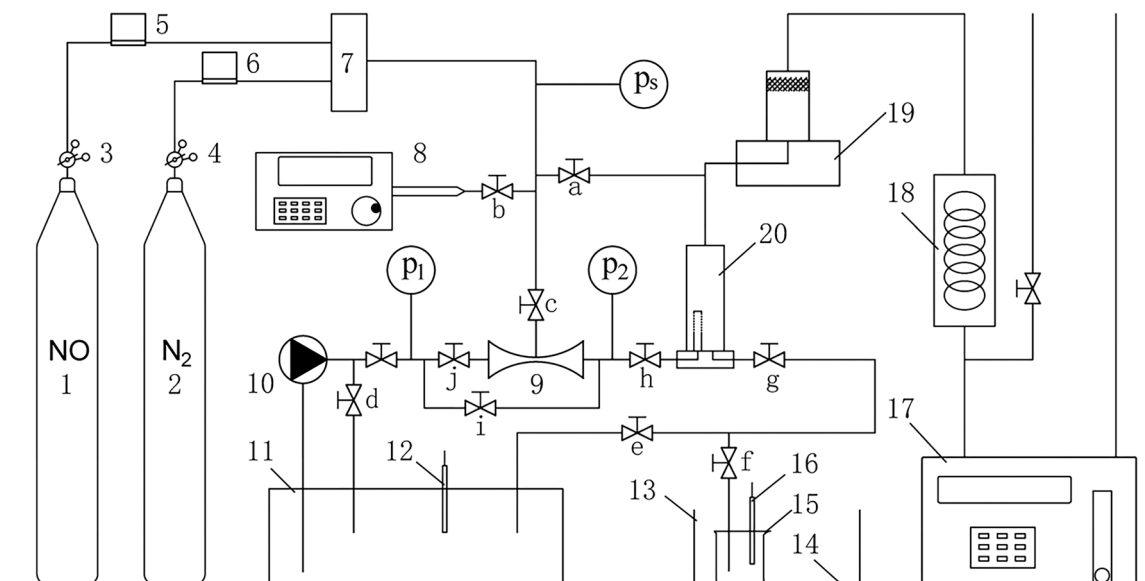
**Fig. 1.** Schematic diagram of experimental system: (1–2) gas cylinders; (3–4) reduced valves; (5–6) mass flow controllers; (7) gas mixer; (8) continuous syringe; (9) HC reactor; (10) pump; (11) constant temperature water bath; (12, 16) pH meter; (13) water tank; (14) drain hole; (15) beaker; (17) gas analyzer; (18) electronic condenser; (19) second stage gas-liquid separator; (20) first stage gas-liquid separator; and (a–j) block valves.

When the solution overflowed in the beaker, it entered the water tank and then flowed through the drain hole to the waste collection point. The samples were sampled through valve f, and the gases were analyzed by the gas analyzer.

### 2.3. Data analysis

When the NO mixture flowed through the HC reactor, the NO reacted with the $ClO_2$ and was removed. The NO removal efficiency is calculated as follows:

$$\eta_{NO} = \left(C_{NO(b)} - C_{NO(a)}\right)/C_{NO(b)} \times 100\% \qquad (1)$$

Where $\eta_{NO}(\%)$ is the NO removal efficiency. $C_{NO(b)}$(ppm) and $C_{NO(a)}$(ppm) are the NO concentrations before and after denitration.

The $NO_x$ removal efficiency is calculated as follows:

$$\eta_{NO_x} = \left(C_{NO_x(b)} - C_{NO_x(a)}\right)/C_{NO_x(b)} \times 100\% \qquad (2)$$

Where $\eta_{NO_x}(\%)$ is the $NO_x$ removal efficiency. $C_{NO_x(b)}$(ppm) and $C_{NO_x(a)}$(ppm) are the $NO_x$ concentrations before and after denitration,

## 3. Results and discussion

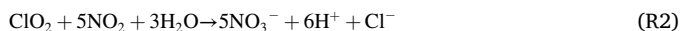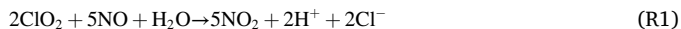### 3.1. The mechanism of HC promoting denitration

#### 3.1.1. The gas-liquid mass transfer was facilitated by the HC reactor

Fig. 2 displayed photographs of bubbles in the first stage gas-liquid separator. The photographs were taken under the same conditions, except for the presence or absence of the HC reactor. The diameters of individual bubbles with and without the HC reactor were about 4 mm and 23 mm. The volume of a single bubble was about 190 times lower due to the presence of the HC reactor. Therefore, the HC reactor could
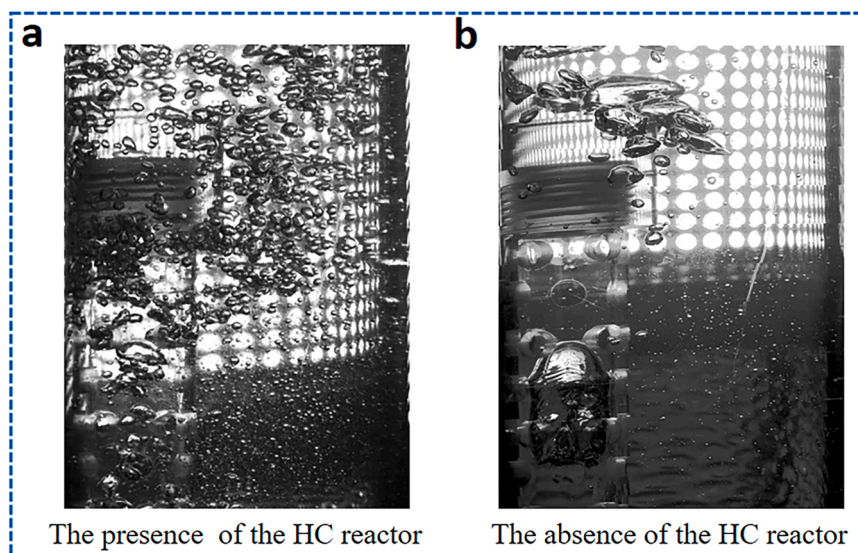


**Fig. 2.** a. Photograph of bubbles in the first stage gas-liquid separator for the solution passing through the HC reactor. b. Photograph of bubbles in the first stage gas-liquid separator for the solution not passing through the HC reactor.

increase the gas-liquid contact area, improving gas-liquid mass transfer. The micro-jets generated by cavitation also enhanced the gas-liquid mass transfer, which further promoted the oxidation of $NO_x$ by the robust oxidant $ClO_2$. $ClO_2$ oxidized NO to $NO_2$, then $NO_2$ was oxidized to nitrate ($NO_3^-$), as shown in (R1) and (R2) [31].

$$2ClO_2 + 5NO + H_2O \rightarrow 5NO_2 + 2H^+ + 2Cl^- \tag{R1}$$

$$ClO_2 + 5NO_2 + 3H_2O \rightarrow 5NO_3^- + 6H^+ + Cl^- \tag{R2}$$

The overall chemical reaction equation for the NO removal could be written as:

$$3ClO_2 + 5NO + 4H_2O \rightarrow 5NO_3^- + 8H^+ + 3Cl^- \tag{R3}$$
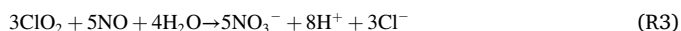
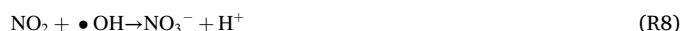### 3.1.2. Gas phase mass transfer was enhanced by the HC reactor

The structure of the HC reactor was shown in the Supplemental Information section, Fig. 1S. When the liquid flowed into the constricted section of the reactor, the liquid flow rate increased, so the kinetic energy of the liquid increased. The pressure energy of the liquid decreased according to the principle of energy conservation. Under low pressure, $ClO_2$ and $H_2O$ molecules volatilized and existed in Gas-Filled-Bubbles. When the fluid passed through the expansion section of the HC reactor, the fluid pressure increased, and the bubbles were compressed and became smaller, promoting intermolecular collisions and improving gas phase mass transfer.

### 3.1.3. Influence of •OH generated by the HC reactor on denitration

Cavitation could cause the pyrolysis of water molecules to generate •OH, according to R4 [47–51].

$$H_2O \rightarrow \bullet OH + \bullet H \tag{R4}$$

$NO_x$ might react with •OH, ultimately transforming to nitrite ($NO_2^-$) and $NO_3^-$, as shown in R5-R8 [52].

$$NO + \bullet OH \rightarrow NO_2^- + H^+ \tag{R5}$$

$$NO + \bullet OH \rightarrow NO_2 + \bullet H \tag{R6}$$

$$2NO_2 + H_2O \rightarrow NO_2^- + NO_3^- + 2H^+ \tag{R7}$$

$$NO_2 + \bullet OH \rightarrow NO_3^- + H^+ \tag{R8}$$

The result of pure water denitration using an HC reactor was shown in the Supplemental Information section, Fig. S2. It could be found from Fig. S2 that the $NO_x$ removal efficiency dropped quickly from 41.0% (70 s) to 31.9% (75 s) in 5 s, which indicated that •OH had no significant effect on NOx removal in this work. The reason might be that the low solubility of NO made it difficult for •OH to contact NO molecules, which made R5 and R6 difficult to occur. Therefore, the improvement of the mass transfer process might be the main reason for the HC reactor to improve the denitration effect of $ClO_2$.
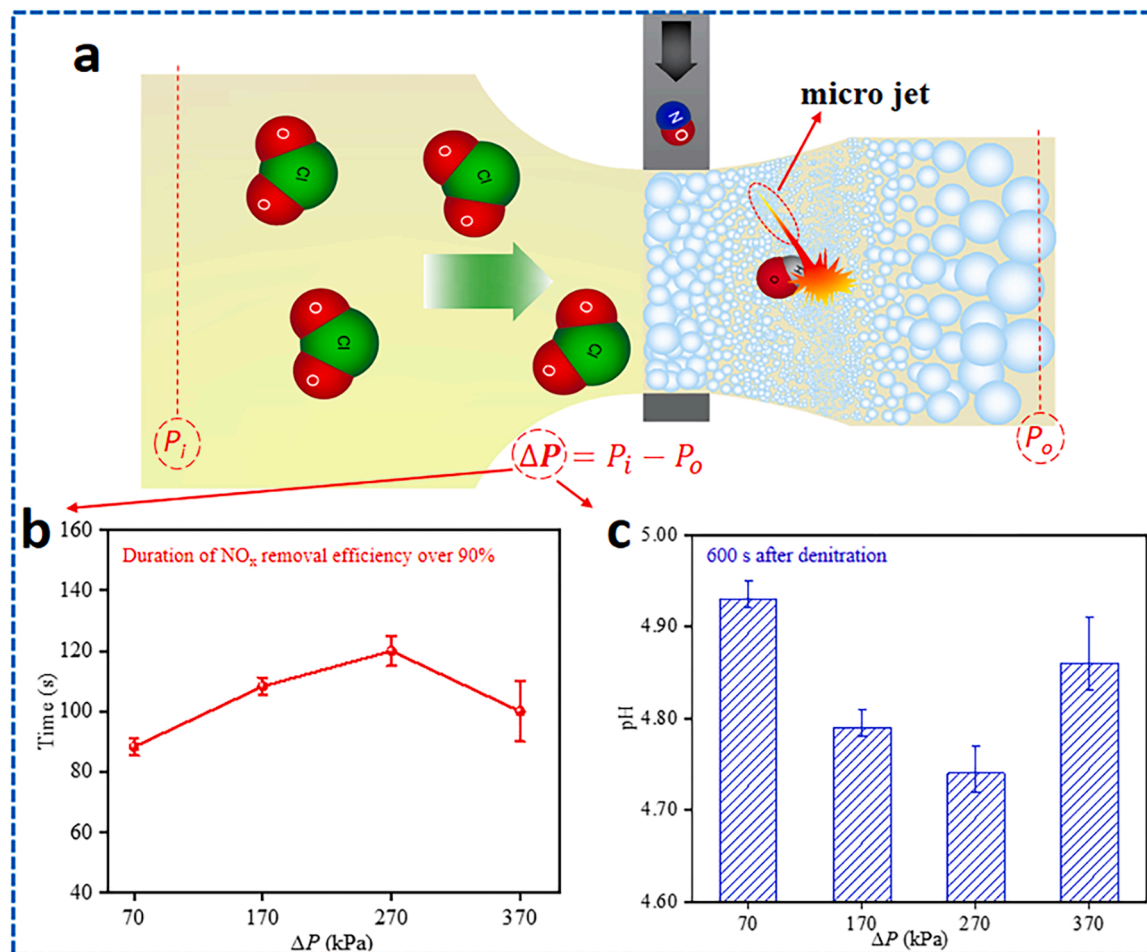


**Fig. 3.** Effect of the $\Delta P$ on $NO_x$ removal. (Conditions: gas flow rate = 1.0 L/min, NO initial concentration 1000 ppm, $ClO_2$ concentration 0.01 mmol/L, solution temperature 25.0 °C.) a. Denitration mechanism of HC enhancing $ClO_2$. b. Variations of the duration for $\eta_{NO_x}$ over 90% with $\Delta P$. c. Variations of solution pH after 600 s denitration with $\Delta P$.

## 3.2. Effect of the $\Delta P$ on denitration

Fig. 3 displayed the effects of the $\Delta P$ on denitration during the HC enhancing $ClO_2$ circulation denitration experiments. The effects of the $\Delta P$ on the denitration effect were presented in Fig. 3b and Fig. 3c when the $P_i$ was 100 kPa, 200 kPa, 300 kPa, 400 kPa, and the $P_o$ remained 30 kPa. The $\Delta P$ was defined as:

$$\Delta P = P_i - P_o \tag{3}$$

Plenty of Gas-Filled-Bubbles could be created by the HC reactor, which extended the gas-liquid contact area. The number and size of the Gas-Filled-Bubbles were affected by cavitation intensity. The cavitation intensity was affected by $\Delta P$ in the experimental process. Cavitation number ($C_v$) could be used to express the cavitation intensity. The smaller $C_v$ might cause a higher cavitation intensity. $C_v$ is calculated as [53,54]:

$$C_v = (P_o - P_v) \Big/ (\frac{1}{2}\rho V_{th}^2) \tag{4}$$

where $P_v$ is the solution's saturated vapor pressure, $V_{th}$ the liquid velocity at the throat of venturi, and $\rho$ the liquid density.

Table 1 indicated that $C_v$ remained about 9.00, 4.00, 2.56, and 1.92 when $\Delta P$ was 70 kPa, 170 kPa, 270 kPa, and 370 kPa. As shown in Fig. 4, the smaller the $C_v$, the larger the Re, and the more intense the turbulence, which would promote the generation of smaller and more bubbles (Fig. 4), expand the gas-liquid contact area, and improve the mass transfer efficiency.

As shown in Fig. 3b, the duration for $\eta_{NO_x}$ over 90% had a first increase followed by a decrease with an increase of $\Delta P$, indicating that there were two reasons. On the one hand, $C_v$ decreased as the $\Delta P$ increased. The cavitation intensity was enhanced, which would aggravate the extreme chemical reaction environment such as high temperature, high pressure, and micro jets produced by cavitation (Fig. 3a). Moreover, with the enhancement of cavitation strength, a stronger micro jet would promote the generation of smaller and more bubbles, which would expand the gas-liquid contact area, and improve the mass transfer efficiency. These improved the denitration effect. On the other hand, $V_{th}$ increased as the $\Delta P$ increased, which would result in a decrease in the total chemical reaction time. These inhibited the denitration effect. When the promoting effect was more significant than the inhibiting effect, the duration for $\eta_{NO_x}$ over 90% increased; otherwise, it decreased. Results showed that the optimal $\Delta P$ was 270 kPa. The experimental result was also confirmed by the relationship of solution pH after 600 s denitration with $\Delta P$. The lowest pH after 600 s denitration was obtained at 270 kPa of $\Delta P$ (Fig. 3c).

## 3.3. Effect of initial solution pH on $NO_x$ removal

Fig. 5 displayed the effect of solution pH on denitration during the HC enhancing $ClO_2$ circulation denitration experiments. Fig. 5a showed that in the range of pH 3–11, the $\eta_{NO_x}$ over 90% could be achieved. The duration for $\eta_{NO_x}$ over 90% decreased with the increase of pH, which might be due to the different chemical reactions in acidic and alkaline media.

As seen in the Supplemental Information section, Fig. 3S, nitrate ($NO_3^-$) and chloride ($Cl^-$) accounted for the majority in the solution

**Table 1**
$C_v$, $V_{th}$ and Liquid flow ($Q_1$) under different $\Delta P$.

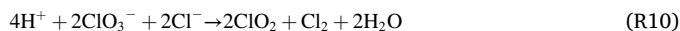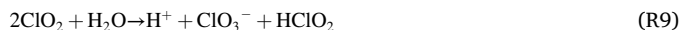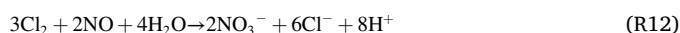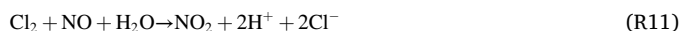| $\Delta P$ (kPa) | $Q_1$ (m³/h) | $V_{th}$ (m/s) | $C_v$ - |
|---|---|---|---|
| 70 | 0.24 | 5.31 | 9.00 |
| 170 | 0.36 | 7.96 | 4.00 |
| 270 | 0.45 | 9.95 | 2.56 |
| 370 | 0.52 | 11.49 | 1.92 |
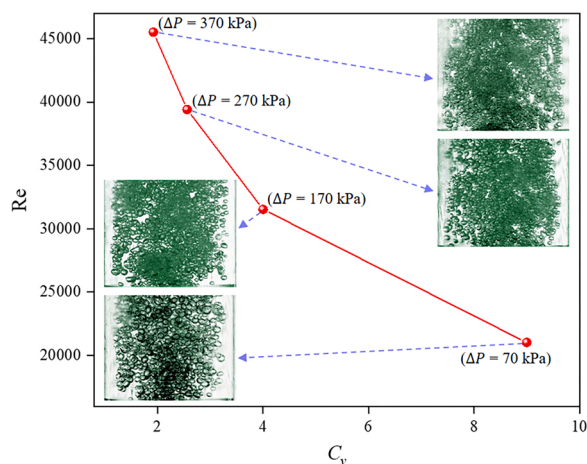


**Fig. 4.** The variation of Re with $C_v$.

after 600 s circulation denitration. The primary process of HC enhancing $ClO_2$ denitration was (R1-R3).

After the disproportionation of a small amount of $ClO_2$, chlorine gas ($Cl_2$) might be produced in an acidic medium, as shown in (R9) and (R10) [21,31,55].
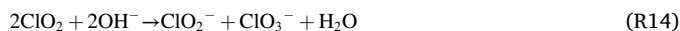
$$2ClO_2 + H_2O \rightarrow H^+ + ClO_3^- + HClO_2 \tag{R9}$$

$$4H^+ + 2ClO_3^- + 2Cl^- \rightarrow 2ClO_2 + Cl_2 + 2H_2O \tag{R10}$$

$Cl_2$ was reactive with NO according to (R11) and (R12) [56].

$$Cl_2 + NO + H_2O \rightarrow NO_2 + 2H^+ + 2Cl^- \tag{R11}$$

$$3Cl_2 + 2NO + 4H_2O \rightarrow 2NO_3^- + 6Cl^- + 8H^+ \tag{R12}$$

The $HClO_2$ could oxidize NO into $NO_3^-$, according to R13.

$$4NO + 3HClO_2 + 2H_2O \rightarrow 4NO_3^- + 3Cl^- + 7H^+ \tag{R13}$$

In an alkaline medium, the disproportionation of $ClO_2$ [44,57] sped up with increasing pH. It led to the formation of chlorite ($ClO_2^-$) and chlorate ($ClO_3^-$), as shown in R14.

$$2ClO_2 + 2OH^- \rightarrow ClO_2^- + ClO_3^- + H_2O \tag{R14}$$

$ClO_2^-$ could remove NO, as shown in R15 and R16 [31].

$$2NO + ClO_2^- \rightarrow 2NO_2 + Cl^- \tag{R15}$$

$$4NO_2 + ClO_2^- + 4OH^- \rightarrow 4NO_3^- + Cl^- + 2H_2O \tag{R16}$$

The overall reaction could be written as:

$$4NO + 3ClO_2^- + 4OH^- \rightarrow 4NO_3^- + 3Cl^- + 2H_2O \tag{R17}$$

It could be seen from (R3) and (R17) that each mole of $ClO_2$ could treat more NO than $ClO_2^-$. So as the pH increased, the duration for $\eta_{NO_x}$ over 90% decreased.

Besides, in an alkaline medium, some $NO_2$ might be absorbed to form $NO_3^-$ and $NO_2^-$, then $NO_2^-$ was oxidized to $NO_3^-$ by $ClO_2$, according to (R18) and (R19).

$$2NO_2 + 2OH^- \rightarrow NO_3^- + NO_2^- + H_2O \tag{R18}$$

$$5NO_2^- + 2ClO_2 + H_2O \rightarrow 5NO_3^- + 2Cl^- + 2H^+ \tag{R19}$$

R18 explained why the highest $NO_2$ concentration decreased with the increase in pH (Fig. 5b).

## 3.4. Effect of solution temperature on $NO_x$ removal

The diffusion behavior, dissolution, and reaction characteristics of
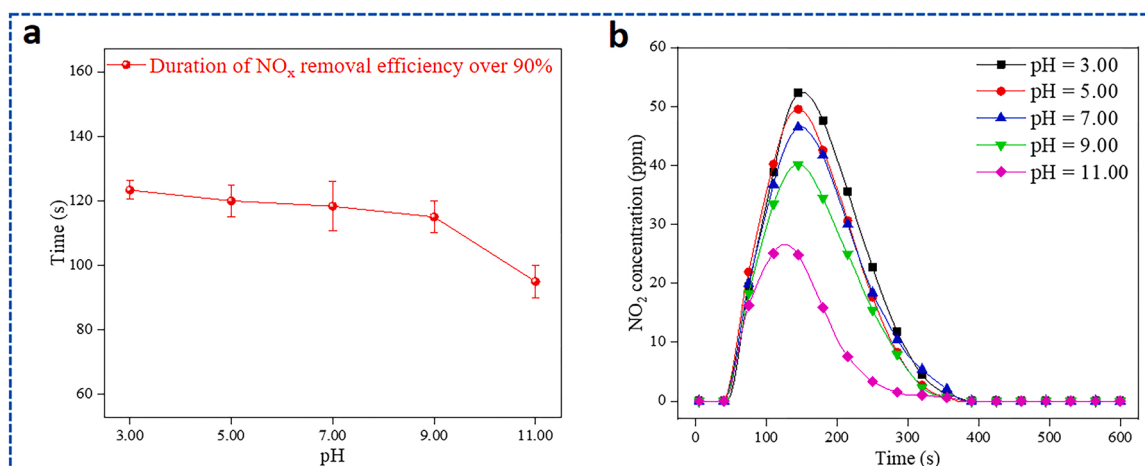
**Fig. 5.** Effect of initial solution pH on denitration. a. Variations of the duration for $\eta_{NO_x}$ over 90% with solution pH. b. Variations of $NO_2$ concentration with time under different initial solution pHs.

molecules or ions in the solution are affected by the reaction temperature [19]. The effect of reaction temperature on $NO_x$ removal was studied experimentally by varying solution temperature from 10.0 °C to 55.0 °C as shown in Fig. 6. From Fig. 6a, the duration for $\eta_{NO_x}$ over 90% had a change of increasing at first and then dropping with the rise of solution temperature. The maximum value of the duration for $\eta_{NO_x}$ over 90% was achieved at 25.0 °C. For this, there were two reasons. On the one hand, The increase in solution temperature will accelerate the diffusion rate of NO and $ClO_2$ molecules, causing an increase in the chemical reaction rates[51]. Meanwhile, $p_v$ increased as the solution temperature increased. Thereby $C_v$ was down. These promoted the denitration effect. On the other hand, the elevated temperature increased the escape rate of $ClO_2$ gas. Meanwhile, An increase in temperature would reduce the solubility of NO and $NO_2$ in aqueous solution [16,19,32]. These inhibited the denitration effect.

Fig. 6b displayed the effect of reaction temperature on the solution pH after 600 s denitration. The denitration solution's initial pH value was about 5.70 in this series of experiments. The solution pH after 600 s denitration was 4.79, 4.74, 4.80, and 4.90. The lowest pH after 600 s denitration was obtained at 25.0 °C. Higher denitration efficiency has lower pH, according to (R3). Thus, 25.0 °C was the optimum solution temperature for HC enhancing $ClO_2$ circulation denitration from 10.0 °C to 55.0 °C.

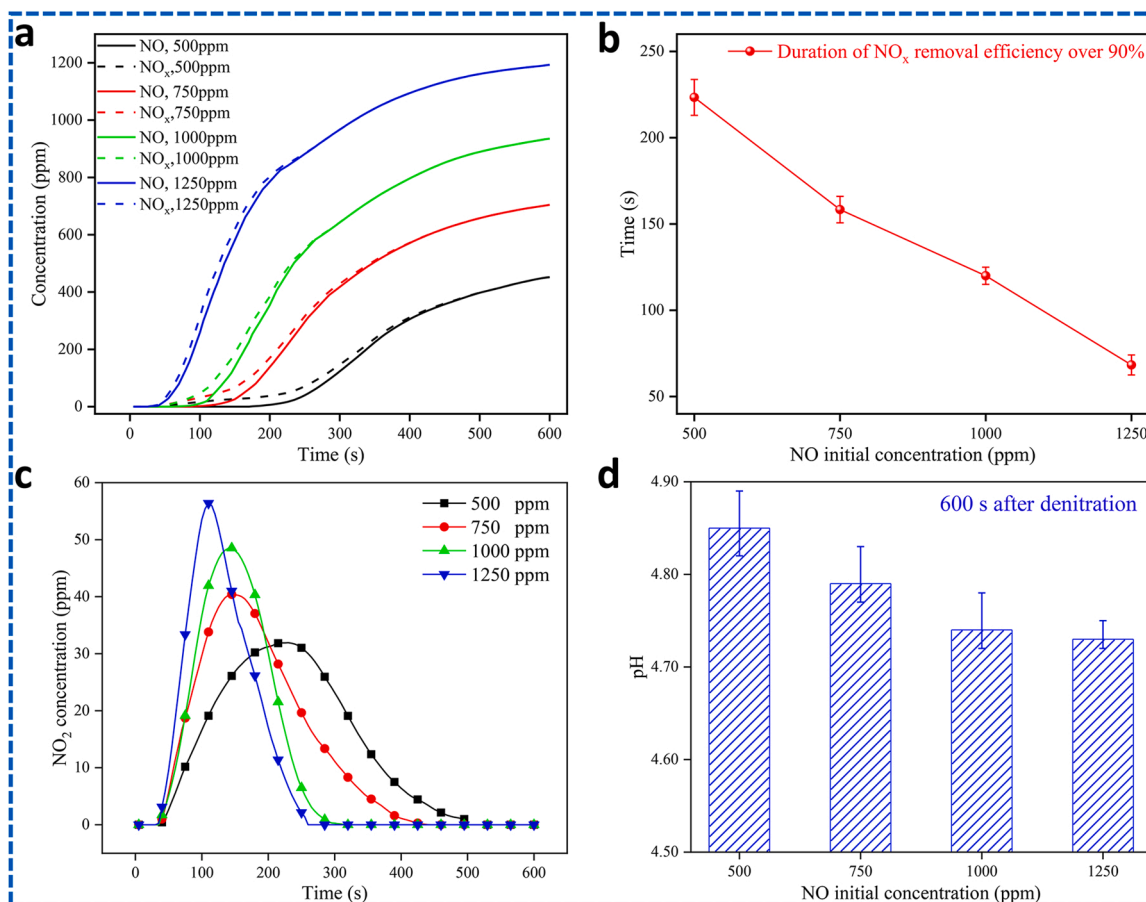### 3.5. Effect of NO initial concentration on $NO_x$ removal

The effect of NO initial concentration on denitration during the HC enhancing $ClO_2$ circulation denitration experiments was shown in Fig. 7. Fig. 7a showed that with the increase of the NO initial concentration, the duration of the NO concentration being 0 ppm gradually decreased. In other words, the higher NO initial concentration led to a shorter duration for $\eta_{NO_x}$ over 90% (Fig. 7b). The NO concentration gradually increased to the near initial NO concentration due to the rapid consumption of $ClO_2$. The curves of NO and $NO_x$ concentrations versus time did not overlap (Fig. 7a) because a small amount of $NO_2$ was produced in the denitration process (Fig. 7c).

Fig. 7d showed the solution pH after 600 s denitration at different NO initial concentrations. The pH of the solution was determined by the amount of $NO_x$ absorbed. The greater the amount of $NO_x$ absorption, the lower the pH. The $NO_x$ absorption was affected by the NO initial concentration and the duration for $\eta_{NO_x}$ over 90%. The longer the duration of the high denitration rate and the higher the initial NO concentration, the more $NO_x$ absorption. Results showed that with the increase of NO initial concentration, the solution pH after 600 s denitration showed a decreasing trend, which was also because the lower initial concentration of NO took longer to consume $ClO_2$ dose in the solution, which caused more $ClO_2$ to overflow. However, when the NO initial concentration increased from 1000 ppm to 1250 ppm, the pH values were almost
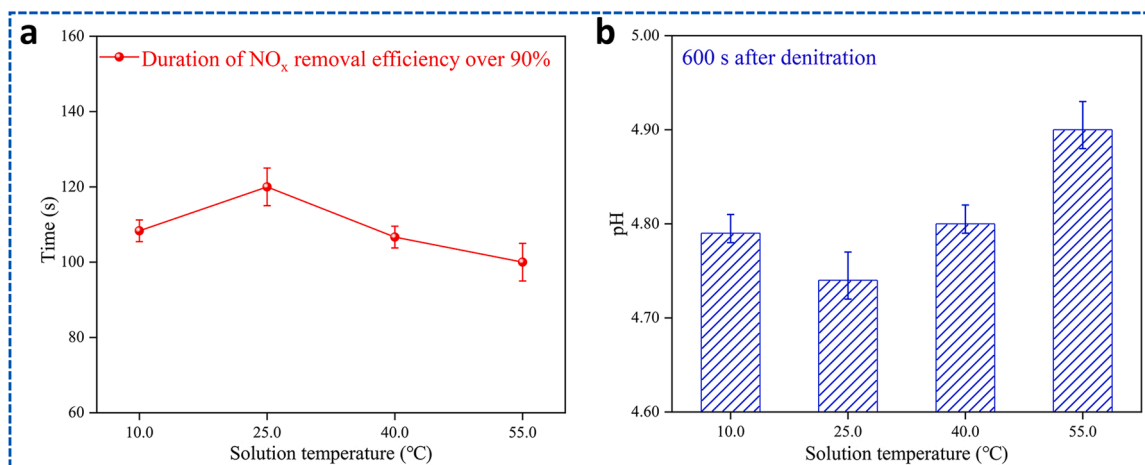


**Fig. 6.** Effect of solution temperature on denitration. (Conditions: gas flow rate 1.0 L/min, NO initial concentration 1000 ppm, $ClO_2$ concentration 0.01 mmol/L, $\Delta P$ 270 kPa) a. Variations of the duration for $\eta_{NO_x}$ over 90% with solution temperature. b. Variations of solution pH after 600 s denitration with solution temperature.
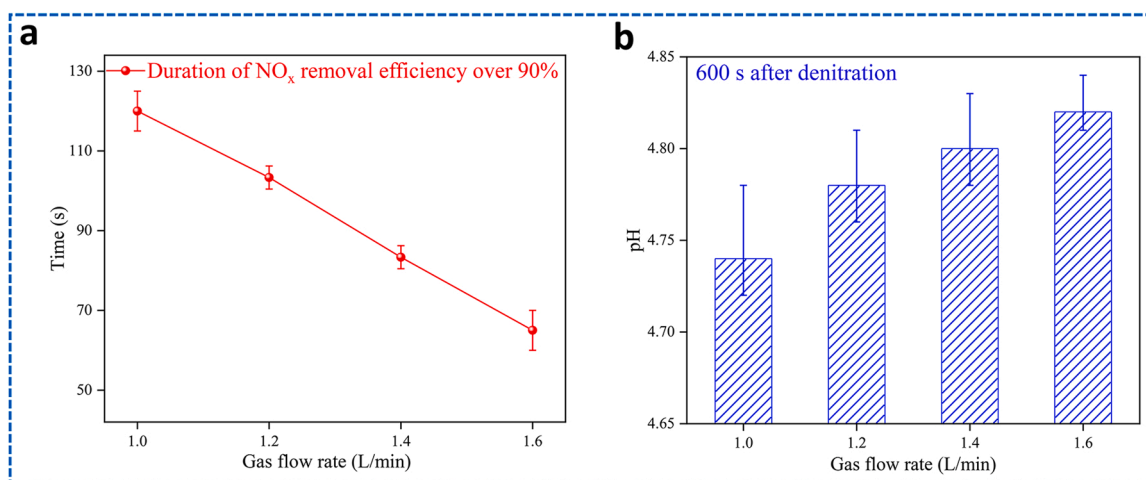
**Fig. 7.** Effect of NO initial concentration on denitration. (Conditions: gas flow rate 1.0 L/min, $ClO_2$ concentration 0.01 mmol/L, solution temperature 25.0 °C, $\Delta P$ 270 kPa) a. Variations of NO concentration and $NO_x$ concentration with time under different NO initial concentrations. b. Variations of the duration for $\eta_{NO_x}$ over 90% with NO initial concentration. c. Variations of $NO_2$ concentration with time under different NO initial concentrations. d. Variations of solution pH after 600 s denitration with NO initial concentration.

equal, which showed that the $ClO_2$ dose in the solution could be almost utilized when the NO initial concentration was 1000 ppm.

### 3.6. Effect of gas flow rate on $NO_x$ removal

The influence of the NO gas flow rate on the denitration effect during the HC enhancing $ClO_2$ circulation denitration experiment was studied. Fig. 8 showed the experimental results. Fig. 8a was the variation of the duration for $\eta_{NO_x}$ over 90% with gas flow rate. The larger the gas flow rate was, the shorter the duration for $\eta_{NO_x}$ over 90% took. Solution pH after 600 s denitration under different gas flow rates in Fig. 8b reflected very interesting results. Although a larger gas flow rate consumed $ClO_2$



**Fig. 8.** Effect of gas flow rate on denitration. (Conditions: NO initial concentration 1000 ppm, $ClO_2$ concentration 0.01 mmol/L, solution temperature 25.0 °C, $\Delta P$ 270 kPa) a. Variations of the duration for $\eta_{NO_x}$ over 90% with gas flow rate. b. Variations of solution pH after 600 s denitration with gas flow rate.

in the solution faster, the lowest pH was obtained when the gas flow rate was 1.0 L/min. It might be because the gas flow rate increased from 1.0 L/min to 1.6 L/min cavitation bubbles were more difficult to collapse, leading to the formation of cavity cloud, which reduced the cavitation intensity[58], resulting in more $ClO_2$ overflows (Table S1). Therefore, the optimal gas flow rate was 1.0 L/min under the experimental conditions.

### 3.7. Effect of initial $ClO_2$ concentration on denitration

Fig. 9 showed the effect of initial $ClO_2$ concentration on $NO_x$ removal during the HC enhancing $ClO_2$ circulation denitration experiments. The increase in initial $ClO_2$ concentration improved the denitration effect. The higher the initial $ClO_2$ concentration was, the longer it took for the $NO_x$ concentration to drop to about 0 (Fig. 9a); namely, the higher the concentration of $ClO_2$ was, the longer duration of $\eta_{NO_x}$ over 90% took, as shown in Fig. 9b (Except for the duration of the initial $ClO_2$ concentration of 0.001 mmol/L). It could be found from Fig. 9b that the duration of pure water denitrification for $\eta_{NO_x}$ over 90% was 40 s, which might be the reason for the experiment design, and the actual effective duration for $\eta_{NO_x}$ over 90% was 0 s. The solution pH was measured continuously during the experiments, and the experimental results were confirmed by the variations of solution pH with time under different $ClO_2$ concentrations. The solution pH after 1800 s denitration remained about 5.91, 4.72, 4.41, 4.30, and 3.78 when the initial $ClO_2$ concentration was 0 mmol/L, 0.01 mmol/L, 0.02 mmol/L, 0.03 mmol/L, and 0.10 mmol/L (Fig. 9c).

There was still $NO_2$ in the gas after denitration, and the concentration of $NO_2$ increased with the initial $ClO_2$ concentration (Fig. 9d). The

escape property of $ClO_2$ could explain this. $NO_2$ was carried by the escape of $ClO_2$, and a higher $ClO_2$ escape rate was caused by a higher initial $ClO_2$ concentration, which led to a higher concentration of $NO_2$. Therefore, a lower initial $ClO_2$ concentration could reduce the production of $NO_2$ and the escape of $ClO_2$ (Table S2). However, the initial $ClO_2$ concentration should not be too low. A too low concentration would not achieve a high denitration effect. As shown in Fig. 9b, when $ClO_2$ concentration was 0.001 mmol/L, the actual effective duration for $\eta_{NO_x}$ over 90% was 0 s, the same as that of $ClO_2$ concentration of 0 mmol/L. Therefore, under the premise of ensuring $\eta_{NO_x}$ over 90%, the lowest possible $ClO_2$ concentration was the best choice. Within the scope of this experiment, 0.010 mmol/L was the best initial $ClO_2$ concentration.

### 3.8. Study on HC enhancing $ClO_2$ non-circulation denitration

During HC enhancing $ClO_2$ circulation denitration, a too-high initial concentration of $ClO_2$ led to too high $NO_2$ concentration after denitration. As shown in Fig. 9d, when the initial concentration of $ClO_2$ was 0.100 mmol/L, the highest concentration of $NO_2$ was 111 ppm. HC enhancing $ClO_2$ non-circulation denitration mode was designed to solve the problem.

#### 3.8.1. The experiment of HC enhancing $ClO_2$ non-circulation denitration
Non-circulation denitration experiments were carried out at solution temperature 25.0 °C, $\Delta P$ 270 kPa, 11.12 mmol/L $ClO_2$ feeding at a rate of 4 ml/min, gas flow rate 1.0 L/min, and NO initial concentration 1000 ppm. As shown in Fig. 10a, the $\eta_{NO}$ and $\eta_{NO_x}$ first increased rapidly and then stabilized at about 93% and 90%, respectively. The variations of solution pH with time also reflected the results of the non-circulation
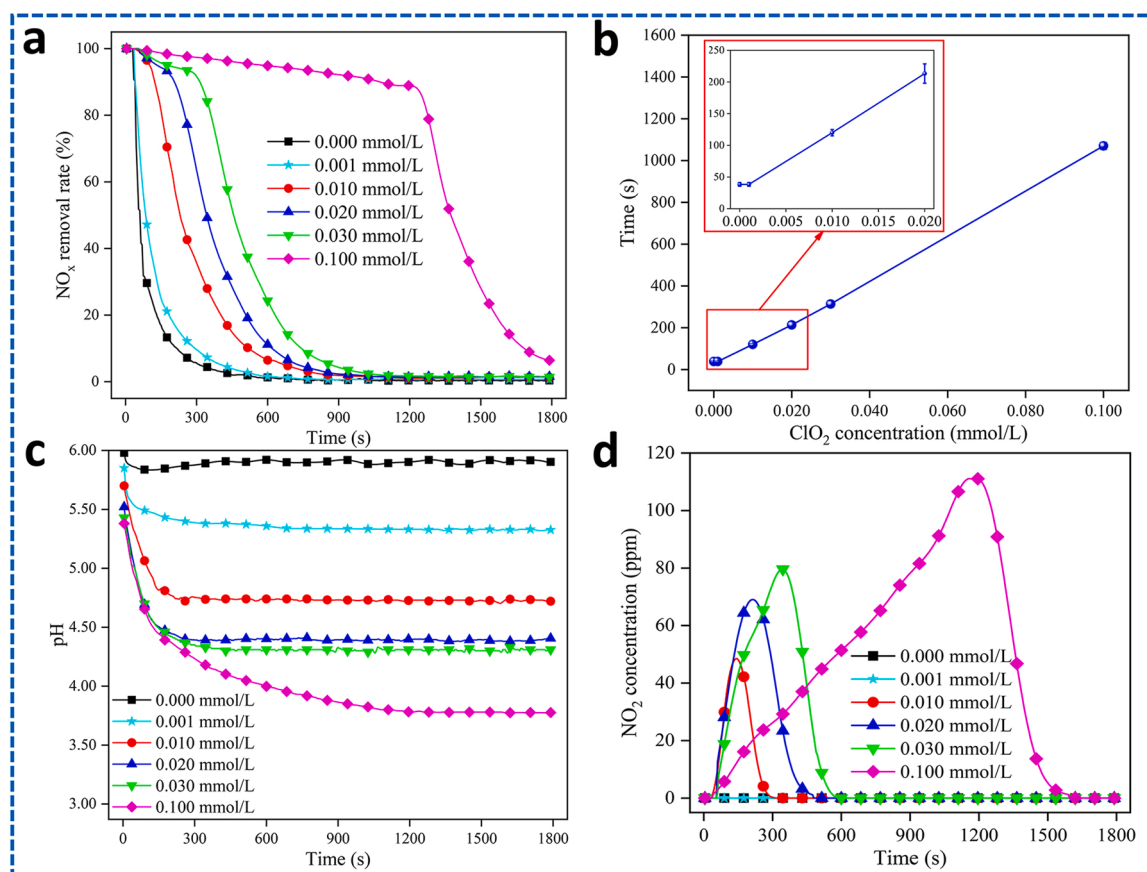


**Fig. 9.** Effect of initial $ClO_2$ concentration on denitration. (Conditions: gas flow rate 1.0 L/min, NO initial concentration 1000 ppm, solution temperature 25.0 °C, $\Delta P$ 270 kPa) a. Variations of $\eta_{NO_x}$ with time under different $ClO_2$ concentrations. b. Variations of the duration for $\eta_{NO_x}$ over 90% with $ClO_2$ concentration. c. Variations of solution pH with time under different $ClO_2$ concentrations. d. Variations of $NO_2$ concentration with time under different $ClO_2$ concentrations.
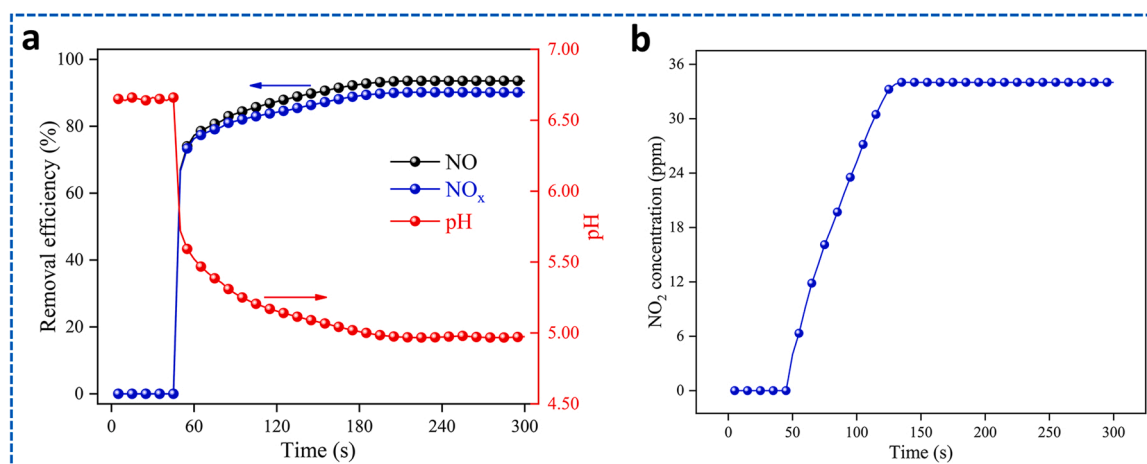
**Fig. 10.** Variations of removal efficiencies and solution pH with time, and $NO_2$ concentration with time. (Conditions: gas flow rate 1.0 L/min, NO initial concentration 1000 ppm, 11.12 mmol/L $ClO_2$ feeding at a rate of 4 ml/min, solution temperature 25.0 °C, $\Delta P$ 270 kPa.).

denitration. One reason for achieving stable and efficient denitration efficiency was that cavitation promoted the occurrence of R1–3. Besides, $NO_x$ might react with •OH, as shown in R5-R8. And then $ClO_2$ would oxidize $NO_2^-$ to $NO_3^-$.

Fig. 10b showed the $NO_2$ concentration with time. $NO_2$ concentration first increased and then stabilized. The highest concentration of $NO_2$ was only 34 ppm. One of the reasons might be R8. HC enhancing $ClO_2$ non-circulation denitration solved the residual $NO_2$ concentration being too high. This research has important guiding significance for the practical application of the one-step HC enhancing $ClO_2$ denitration method.

*3.8.2. Analysis of anions on denitration*

We took samples at an interval of 40 s, and Fig. 11 showed the analysis results of anion products containing nitrogen atoms in the samples. It could be found from Fig. 11 that the anion product containing nitrogen atoms was only $NO_3^-$ after 280 s non-circulation denitration, which meant that most of the absorbed $NO_x$ were converted to $NO_3^-$. The $NO_3^-$ was the natural composition of seawater and was non-polluting to the ocean. We did not detect $NO_2^-$, which was very toxic [59]. It was also observed that the trend of the measured values and the theoretical ones was the same.

## 4. Conclusions

We carried out a detailed study to check the effects of various parameters on denitration using HC enhancing $ClO_2$. Results showed that the HC reactor mainly enhanced the mass transfer process to enhance the removal of $NO_x$ by $ClO_2$. In a wide pH range of 3–11, the $\eta_{NO_x}$ was more than 90% during the HC enhancing $ClO_2$ circulation denitration experiments. The duration for $\eta_{NO_x}$ over 90% initially increased to a maximum value and then decreased with the rise of operating conditions like solution temperature and $\Delta P$. The duration for $\eta_{NO_x}$ over 90% decreased with increasing NO initial concentration and gas flow rate and increased with increasing initial $ClO_2$ concentration. Considering the application to the practical engineering, based on the results of HC enhancing $ClO_2$ circulation denitration, the HC enhancing $ClO_2$ non-circulation denitration experiment was carried out under conditions of gas flow rate 1.0 L/min, NO initial concentration 1000 ppm, $\Delta P$ 270 kPa, solution temperature 25 °C, and 11.12 mmol/L $ClO_2$ feeding at a rate of 4 ml/min. The results showed that $\eta_{NO}$ and $\eta_{NO_x}$ reached 93% and 90%, respectively. The $NO_3^-$ was the only final product of denitration and was non-polluting to the ocean. The research findings showed that the HC enhancing $ClO_2$ denitration method had huge potential for industrial application in flue gas cleaning.
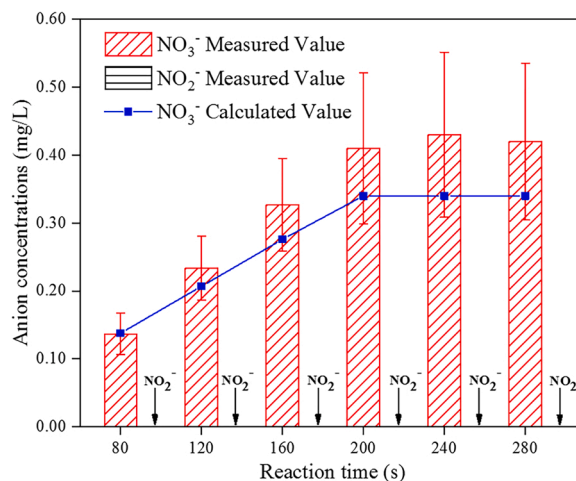


**Fig. 11.** Analysis of anion products containing nitrogen atoms in the samples. (Conditions: gas flow rate 1.0 L/min, NO initial concentration 1000 ppm, 11.12 mmol/L $ClO_2$ feeding at a rate of 4 ml/min, solution temperature 25.0 °C, $\Delta P$ 270 kPa.).

## Credit author statement

**Jingang Yang:** Conceptualization, Methodology, Data curation, Writing – original draft, Investigation, Writing – review & editing. **Liguo Song:** Conceptualization, Methodology, Data curation, Writing – original draft, Investigation, Supervision, Writing – review & editing. **Yuhang Wei:** Investigation, Validation, Writing – review & editing. **Hao Sui:** Investigation, Validation, Writing – review & editing. **Chengqi Deng:** Investigation, Validation, Writing – review & editing. **Bohao Zhang:** Investigation, Writing – review & editing. **Kaixuan Lu:** Investigation, Writing – review & editing. **Minyi Xu:** Supervision, Writing – review & editing. **Zhitao Han:** Supervision, Writing – review & editing. **Xinxiang Pan:** Supervision, Writing – review & editing.

## Acknowledgments

## Appendix A. Supporting information

Supplementary data associated with this article can be found in the online version at doi:10.1016/j.jece.2022.107897.

## References

[1] G. Mallouppas, E.A. Yfantis, Decarbonization in shipping industry: a review of research, technology development, and innovation proposals, J. Mar. Sci. Eng. 9 (2021) 415, https://doi.org/10.3390/jmse9040415.

[2] C.G. Rodríguez, M.I. Lamas, J.D.D. Rodríguez, A. Abbas, Possibilities of ammonia as both fuel and NOx reductant in marine engines: a numerical study, J. Mar. Sci. Eng 10 (2022) 43, https://doi.org/10.3390/jmse10010043.

[3] T. Stavrakou, J.-F. Müller, M. Bauwens, K.F. Boersma, J. Van Geffen, Satellite evidence for changes in the $NO_2$ weekly cycle over large cities, Sci. Rep. 10 (2020) 10066, https://doi.org/10.1038/s41598-020-66891-0.

[4] P. Chen, Research on desulfurization and denitration technologies of ship exhaust, IOP Conf. Ser. Earth Environ. Sci. 450 (2020), 012111, https://doi.org/10.1088/1755-1315/450/1/012111.

[5] M. Sofiev, J.J. Winebrake, L. Johansson, E.W. Carr, M. Prank, J. Soares, J. Vira, R. Kouznetsov, J.-P. Jalkanen, J.J. Corbett, Cleaner fuels for ships provide public health benefits with climate tradeoffs, Nat. Commun. 9 (2018) 406, https://doi.org/10.1038/s41467-017-02774-9.

[6] Z. Xiao, D. Li, Q. Zhu, Z. Sun, Simultaneous removal of NO and $SO_2$ through a new wet recycling oxidation–reduction process utilizing micro-nano bubble gas–liquid dispersion system based on $Na_2SO_3$, Fuel 263 (2020), 116682, https://doi.org/10.1016/j.fuel.2019.116682.

[7] Z. Xiao, D. Li, Simultaneous removal of NO and $SO_2$ with a micro-bubble gas-liquid dispersion system based on air/$H_2O_2$/$Na_2S_2O_8$, Environ. Technol. (2019), https://doi.org/10.1080/09593330.2019.1615134.

[8] T. Makkonen, S. Repka, The innovation inducement impact of environmental regulations on maritime transport: a literature review, Int. J. Innov. Sustain. Dev. 10 (2016) 69–86, https://doi.org/10.1504/IJISD.2016.073413.

[9] S. Mohan, P. Dinesha, S. Kumar, NOx reduction behaviour in copper zeolite catalysts for ammonia SCR systems: a review, Chem. Eng. J. 384 (2020) 123253, https://doi.org/10.1016/j.cej.2019.123253.

[10] B. Guan, R. Zhan, H. Lin, Z. Huang, Review of state of the art technologies of selective catalytic reduction of $NO_x$ from diesel engine exhaust, Appl. Therm. Eng. 66 (2014) 395–414, https://doi.org/10.1016/j.applthermaleng.2014.02.021.

[11] T.V.W. Janssens, H. Falsig, L. Lundegaard, P. Vennestrøm, S. Rasmussen, P. Moses, F. Giordanino, E. Borfecchia, K. Lomachenko, C. Lamberti, S. Bordiga, A. Godiksen, S. Mossin, P. Beato, A consistent reaction scheme for the selective catalytic reduction of nitrogen oxides with ammonia, ACS Catal. 5 (2015) 2832–2845, https://doi.org/10.1021/cs501673g.

[12] U. Asad, M. Zheng, Exhaust gas recirculation for advanced diesel combustion cycles, Appl. Energy 123 (2014) 242–252, https://doi.org/10.1016/j.apenergy.2014.02.073.

[13] P.S. Divekar, X. Chen, J. Tjong, M. Zheng, Energy efficiency impact of EGR on organizing clean combustion in diesel engines, Energy Convers. Manag. 112 (2016) 369–381, https://doi.org/10.1016/j.enconman.2016.01.042.

[14] G. Fontana, E. Galloni, Experimental analysis of a spark-ignition engine using exhaust gas recycle at WOT operation, Appl. Energy 87 (2010) 2187–2193, https://doi.org/10.1016/j.apenergy.2009.11.022.

[15] R.T. Guo, J.K. Hao, W.G. Pan, Y.L. Yu, Liquid phase oxidation and absorption of NO from flue gas: a review, Sep Sci Technol 50 (2015) 310–321, https://doi.org/10.1080/01496395.2014.956761.

[16] M.S. Kang, J. Shin, T.U. Yu, J. Hwang, Simultaneous removal of gaseous $NO_x$ and $SO_2$ by gas-phase oxidation with ozone and wet scrubbing with sodium hydroxide, Chem. Eng. J. 381 (2020) 122601, https://doi.org/10.1016/j.cej.2019.122601.

[17] F.X. Hu, G.H. Yang, H. Xiang, Z.F. Hu, Y.Y. Cui, S.R. Tian, DeNOx performance of a compact SCR catalyst on marine diesel engine, Chin. J. Eng. Des 10 (2016) 3130–3134, https://doi.org/10.12030/j.cjee.201509098.

[18] D. Agarwal, S.K. Singh, A.K. Agarwal, Effect of exhaust gas recirculation (EGR) on performance, emissions, deposits and durability of a constant speed compression ignition engine, Appl. Energy 88 (2011) 2900–2907, https://doi.org/10.1016/j.apenergy.2011.01.066.

[19] P. Fang, C.P. Cen, Z.X. Tang, P.Y. Zhong, D.S. Chen, Z.H. Chen, Simultaneous removal of $SO_2$ and $NO_x$ by wet scrubbing using urea solution, Chem. Eng. J 168 (2011) 52–59, https://doi.org/10.1016/j.cej.2010.12.030.

[20] T.W. Chien, H. Chu, Removal of $SO_2$ and NO from flue gas by wet scrubbing using an aqueous $NaClO_2$ solution, J. Hazard. Mater. 80 (2000) 43–57, https://doi.org/10.1016/S0304-3894(00)00274-0.

[21] D.S. Jin, B.R. Deshwal, Y.S. Park, H.K. Lee, Simultaneous removal of $SO_2$ and NO by wet scrubbing using aqueous chlorine dioxide solution, J. Hazard. Mater. 135 (2006) 412–417, https://doi.org/10.1016/j.jhazmat.2005.12.001.

[22] Y. Zhao, T.X. Guo, Z.Y. Chen, Y.R. Du, Simultaneous removal of $SO_2$ and NO using M/$NaClO_2$ complex absorbent, Chem. Eng. J. 160 (2010) 42–47, https://doi.org/10.1016/j.cej.2010.02.060.

[23] A.H. Hultén, P. Nilsson, M. Samuelsson, S. Ajdari, F. Normann, K. Andersson, First evaluation of a multicomponent flue gas cleaning concept using chlorine dioxide gas – experiments on chemistry and process performance, Fuel 210 (2017) 885–891, https://doi.org/10.1016/j.fuel.2017.08.116.

[24] Z. Xiao, D. Li, F. Wang, Z. Sun, Z. Lin, Simultaneous removal of NO and $SO_2$ with a new recycling micro-nano bubble oxidation-absorption process based on HA-Na, Sep. Purif. Technol. 242 (2020), 116788, https://doi.org/10.1016/j.seppur.2020.116788.

[25] Z. Xiao, T.B. Aftab, D. Li, Applications of micro–nano bubble technology in environmental pollution control, Micro Nano Lett. 14 (2019) 782–787, https://doi.org/10.1049/mnl.2018.5710.

[26] Z. Xiao, D. Li, R. Zhang, F. Wang, F. Pan, Z. Sun, An experimental study on the simultaneous removal of NO and $SO_2$ with a new wet recycling process based on the micro-nano bubble water system, Environ. Sci. Pollut. Res. 27 (2020) 4197–4205, https://doi.org/10.1007/s11356-019-07136-0.

[27] Y.-Y. Mao, H.-Y. Wang, P.-S. Sun, P. Zou, L.-Q. Dong, J. Wang, X.-Y. Bi, F.-T. Deng, X.-Y. Zheng, Study on biological simultaneous removal of $SO_2$ and $NO_x$ from high temperature flue gas by biological trickling filter, J. Yunnan Univ. Nat. Sci. Ed. 34 (2012) 227–231.

[28] A. Sepehri, M.-H. Sarrafzadeh, Activity enhancement of ammonia-oxidizing bacteria and nitrite-oxidizing bacteria in activated sludge process: metabolite reduction and $CO_2$ mitigation intensification process, Appl. Water Sci. 9 (2019) 1–12, https://doi.org/10.1007/s13201-019-1017-6.

[29] A. Sepehri, M.-H. Sarrafzadeh, Effect of nitrifiers community on fouling mitigation and nitrification efficiency in a membrane bioreactor, Chem. Eng. Process. 128 (2018) 10–18, https://doi.org/10.1016/j.cep.2018.04.006.

[30] A. Sepehri, M.-H. Sarrafzadeh, M. Avateffazeli, Interaction between Chlorella vulgaris and nitrifying-enriched activated sludge in the treatment of wastewater with low C/N ratio, J. Clean. Prod. 247 (2020) 119164, https://doi.org/10.1016/j.jclepro.2019.119164.

[31] B.R. Deshwal, D.S. Jin, S.H. Lee, S.H. Moon, J.H. Jung, H.K. Lee, Removal of NO from flue gas by aqueous chlorine-dioxide scrubbing solution in a lab-scale bubbling reactor, J. Hazard. Mater. 150 (2008) 649–655, https://doi.org/10.1016/j.jhazmat.2007.05.016.

[32] B.R. Deshwal, S.H. Lee, J.H. Jung, B.H. Shon, H.K. Lee, Study on the removal of $NO_x$ from simulated flue gas using acidic $NaClO_2$ solution, J. Environ. Sci. 20 (2008) 33–38, https://doi.org/10.1016/S1001-0742(08)60004-2.

[33] Y.T. Didenko, W.B. Mcnamara, K.S. Suslick, Hot spot conditions during cavitation in water, J. Am. Chem. Soc. 121 (1999) 5817–5818, https://doi.org/10.1021/ja9844635.

[34] K.S. Suslick, Sonochemistry, Science 247 (1990) 1439–1445, https://doi.org/10.1126/science.247.4949.1439.

[35] K.S. Suslick, N.C. Eddingsaas, D.J. Flannigan, S.D. Hopkins, H. Xu, The chemical history of a bubble, Acc. Chem. Res. 51 (2018) 2169–2178, https://doi.org/10.1021/acs.accounts.8b00088.

[36] S.Z. You, M.W. Chen, D.D. Dlott, K.S. Suslick, Ultrasonic hammer produces hot spots in solids, Nat. Commun. 6 (2015) 6581, https://doi.org/10.1038/ncomms7581.

[37] I. Kim, I. Lee, S.H. Jeon, T. Hwang, J.-I. Han, Hydrodynamic cavitation as a novel pretreatment approach for bioethanol production from reed, Bioresour. Technol. 192 (2015) 335–339, https://doi.org/10.1016/j.biortech.2015.05.038.

[38] V. Innocenzi, M. Prisciandaro, M. Centofanti, F. Vegliò, Comparison of performances of hydrodynamic cavitation in combined treatments based on hybrid induced advanced Fenton process for degradation of azo-dyes, J. Environ. Chem. Eng. 7 (2019), 103171, https://doi.org/10.1016/j.jece.2019.103171.

[39] R.P. Taleyarkhan, C.D. West, J.S. Cho, R.T. Lahey, R.I. Nigmatulin, R.C. Block, Evidence for nuclear emissions during acoustic cavitation, Science 295 (2002) 1868–1873, https://doi.org/10.1126/science.1067589.

[40] D. Musmarra, M. Prisciandaro, M. Capocelli, D. Karatza, P. Iovino, S. Canzano, A. Lancia, Degradation of ibuprofen by hydrodynamic cavitation: reaction pathways and effect of operational parameters, Ultrason. Sonochem. 29 (2016) 76–83, https://doi.org/10.1016/j.ultsonch.2015.09.002.

[41] N.S. Srinivas, K.K. Ramanan, J.B.B. Rayappan, N.J. Kaleekkal, G.B. Jegadeesan, Coumarin as a chemical probe to evaluate efficiency of vortex–based hydrodynamic cavitation process, J. Environ. Chem. Eng. 10 (2022), 106940, https://doi.org/10.1016/j.jece.2021.106940.

[42] A. Bokhari, L.F. Chuah, S. Yusup, J.J. Klemeš, M.M. Akbar, R.N.M. Kamil, Cleaner production of rubber seed oil methyl ester using a hydrodynamic cavitation: optimisation and parametric study, J. Clean. Prod. 136 (2016) 31–41, https://doi.org/10.1016/j.jclepro.2016.04.091.

[43] A. Bokhari, L.F. Chuah, S. Yusup, J.J. Klemeš, R.N.M. Kamil, Optimisation on pretreatment of rubber seed (Hevea brasiliensis) oil via esterification reaction in a hydrodynamic cavitation reactor, Bioresour. Technol. 199 (2016) 414–422, https://doi.org/10.1016/j.biortech.2015.08.013.

[44] Y. Sun, W.K. Niu, X.J. Hu, X.H. Ma, Y.J. Sun, Y. Wen, Oxidative degradation of polycyclic aromatic hydrocarbons in contaminated industrial soil using chlorine dioxide, Chem. Eng. J. 394 (2020), 124857, https://doi.org/10.1016/j.cej.2020.124857.

[45] G. Hey, R. Grabic, A. Ledin, J.L.C. Jansen, H.R. Andersen, Oxidation of pharmaceuticals by chlorine dioxide in biologically treated wastewater, Chem. Eng. J. 185–186 (2012) 236–242, https://doi.org/10.1016/j.cej.2012.01.093.

[46] F.X. Tian, B. Xu, T.Y. Zhang, N.Y. Gao, Degradation of phenylurea herbicides by chlorine dioxide and formation of disinfection by-products during subsequent chlor (am)ination, Chem. Eng. J. 258 (2014) 210–217, https://doi.org/10.1016/j.cej.2014.07.094.

[47] A.L. Prajapat, P.R. Gogate, Intensified depolymerization of aqueous polyacrylamide solution using combined processes based on hydrodynamic cavitation, ozone, ultraviolet light and hydrogen peroxide, Ultrason. Sonochem. 31 (2016) 371–382, https://doi.org/10.1016/j.ultsonch.2016.01.021.

[48] J.L. Wang, L.J. Xu, Advanced oxidation processes for wastewater treatment: formation of hydroxyl radical and application, Crit. Rev. Environ. Sci. Technol. 42 (2012) 251–325, https://doi.org/10.1080/10643389.2010.507698.

[49] N.B. Suryawanshi, V.M. Bhandari, L.G. Sorokhaibam, V.V. Ranade, A non-catalytic deep desulphurization process using hydrodynamic cavitation, Sci. Rep. 6 (2016) 33021, https://doi.org/10.1038/srep33021.

[50] M.P. Badve, P.R. Gogate, A.B. Pandit, L. Csoka, Hydrodynamic cavitation as a novel approach for delignification of wheat straw for paper manufacturing, Ultrason. Sonochem. 21 (2014) 162–168, https://doi.org/10.1016/j.ultsonch.2013.07.006.

[51] P.R. Gogate, P.N. Patil, Combined treatment technology based on synergism between hydrodynamic cavitation and advanced oxidation processes, Ultrason. Sonochem. 25 (2015) 60–69, https://doi.org/10.1016/j.ultsonch.2014.08.016.

[52] Y.G. Adewuyi, Sonochemistry: environmental science and engineering applications, Ind. Eng. Chem. Res. 40 (2001) 4681–4715, https://doi.org/10.1021/ie010096l.

[53] P.S. Kumar, A.B. Pandit, Modeling hydrodynamic cavitation, Chem. Eng. Technol. 22 (1999) 1017–1027, https://doi.org/10.1002/(SICI)1521-4125(199912)22:12<1017::AID-CEAT1017>3.0.CO;2-L.

[54] A. Šarc, T. Stepišnik-Perdih, M. Petkovšek, M. Dular, The issue of cavitation number value in studies of water treatment by hydrodynamic cavitation, Ultrason. Sonochem. 34 (2017) 51–59, https://doi.org/10.1016/j.ultsonch.2016.05.020.

[55] B. Deshwal, H.-K. Lee, Kinetics and mechanism of chloride based chlorine dioxide generation process from acidic sodium chlorate, J. Hazard. Mater. 108 (2004) 173–182, https://doi.org/10.1016/j.jhazmat.2003.12.006.

[56] C.L. Yang, H. Shaw, H.D. Perlmutter, Absorption of NO promoted by strong oxidizing agents: 1. Inorganic oxychlorites in nitric acid, Chem. Eng. Commun. 143 (1996) 23–38, https://doi.org/10.1080/00986449608936432.

[57] J.F. White, M.C. Taylor, G.P. Vincent, Chemistry of chlorites, Ind. Eng. Chem. 34 (1942) 782–792, https://doi.org/10.1021/ie50391a003.

[58] P. Thanekar, M. Panda, P.R. Gogate, Degradation of carbamazepine using hydrodynamic cavitation combined with advanced oxidation processes, Ultrason. Sonochem. 40 (2018) 567–576, https://doi.org/10.1016/j.ultsonch.2017.08.001.

[59] Y.G. Adewuyi, S.O. Owusu, Aqueous absorption and oxidation of nitric oxide with oxone for the treatment of tail gases: process feasibility, stoichiometry, reaction pathways, and absorption rate, Ind. Eng. Chem. Res. 42 (2003) 4084–4100, https://doi.org/10.1021/ie020709.